ELSEVIER

Biochimica et Biophysica Acta 1502 (2000) 16–30

BIOCHIMICA ET BIOPHYSICA ACTA
BBA

www.elsevier.com/locate/bba

Review

Alzheimer's amyloid fibrils: structure and assembly

Louise C. Serpell *

Neurobiology Division, MRC Centre, Laboratory of Molecular Biology, Hills Road, Cambridge CB2 2QH, UK

Received 16 June 1999; received in revised form 24 November 1999; accepted 24 November 1999

Abstract

Structural studies of Alzheimer's amyloid fibrils have revealed information about the structure at different levels. The amyloid-β peptide has been examined in various solvents and conditions and this has led to a model by which a conformational switching occurs from α-helix or random coil, to a β-sheet structure. Amyloid fibril assembly proceeds by a nucleation dependent pathway leading to elongation of the fibrils. Along this pathway small oligomeric intermediates and short fibrillar structures (protofibrils) have been observed. In cross-section the fibril appears to be composed of several subfibrils or protofilaments. Each of these protofilaments is composed of β-sheet structure in which hydrogen bonding occurs along the length of the fibre and the β-strands run perpendicular to the fibre axis. This hierarchy of structure is discussed in this review.

Keywords: Amyloid; Alzheimer's disease; Structure; Fibril; Beta-sheet

1. Introduction

Alzheimer's disease is characterised by the deposition of insoluble amyloid fibrils as amyloid plaques in the neuropil as well as the accumulation of neurofibrillary tangles in cell bodies of neurones [1]. The amyloid fibrils are composed of the amyloid-β peptide (Aβ), a 39–43 amino acid residue peptide produced by cleavage from a larger amyloid precursor protein, APP. The Aβ peptide is known to be present in unaffected individuals and is thought to have a normal physiological role. However, in Alzheimer's disease patients the Aβ peptide forms ordered aggregates which are deposited extracellularly as amyloid plaques or senile plaques in the neuropil, and as vascular deposits.

Alzheimer's disease is not the only disease in which amyloid fibrils are involved in the pathology. There is now a list of some 16 proteins which can form amyloid fibrils in various diseases [2,3]. These proteins vary considerably in their primary structure, function, size and tertiary structure, and yet they appear to form amyloid fibrils which show very few structural differences. Electron microscopy has shown [4,5] that amyloid fibrils are straight, unbranching fibres of 70–120 Å in diameter and of indeterminate length. An electron micrograph of Aβ1–40 amyloid fibrils formed in vitro is shown in Fig. 1. All amyloid fibrils stain with the dye Congo red and give a green birefringence when examined under cross-polarised light, and finally they reveal a cross-β fibre diffraction pattern which suggests a β-sheet type structure for the fibrils [3,6]. The nature of the diffraction pattern and its interpretation are illustrated in Fig. 2.

Structural studies of amyloid fibrils from Alzheim-

* Fax: +44-1223-402310;
E-mail: serpell@mrc-lmb.cam.ac.uk

0925-4439/00/$ – see front matter
PII: S0925-4439(00)00029-6

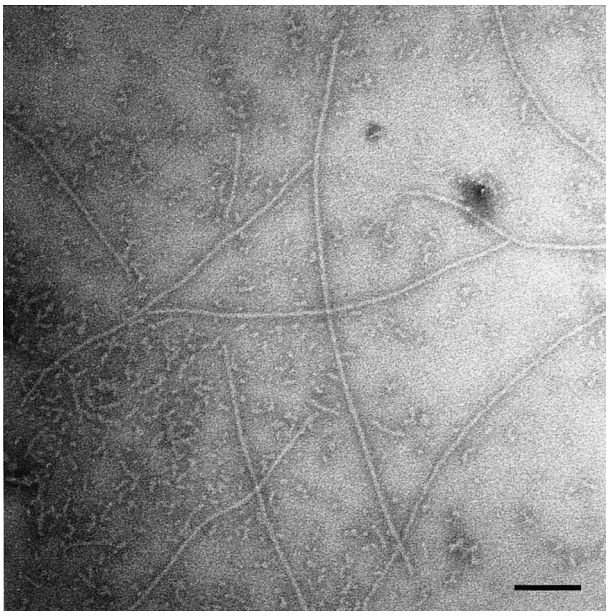

Fig. 1. Electron micrograph of amyloid fibrils formed in water from Aβ1–42, stained with 0.1% phosphotungstic acid (Serpell, unpublished results) showing long straight fibrils of 70–80 Å diameter as well as fibrillar aggregate background. Bar = 1000 Å.

er's disease brain have proved extremely difficult due to the insolubility of the plaques. Examination of the structure of amyloid has concentrated on amyloid fibrils formed in vitro from synthetic peptides homologous to the Aβ peptide. Peptide fragments of Aβ form amyloid fibrils in vitro which have a similar, if not identical, morphology [7–11] and immunoreactivity to in situ Alzheimer's disease amyloid [7]. However, even synthetic amyloid fibrils are problematic to study using conventional structural techniques. Methods such as single crystal X-ray crystallography and solution nuclear magnetic resonance (NMR) cannot be used on fibrils since they are insoluble. Therefore X-ray fibre diffraction, electron microscopy (EM), solid state NMR, Fourier transform infrared spectroscopy (FTIR) and circular dichroism (CD) have been used to examine amyloid structure. These techniques have yielded considerable information about the morphology of amyloid fibrils and their internal structural conformation. However, we have yet to obtain an unambiguous structure of the amyloid fibril. In this review I will endeavour to discuss all the work that has led to a picture of amyloid fibril as it now stands.

The field of structural studies of Aβ amyloid is extremely complex and encompasses the structure of the soluble Aβ peptide, its polymerisation into intermediates and from intermediates to amyloid fibrils, to the fibrils themselves and finally to amyloid deposition in vivo. Structural studies of soluble Aβ

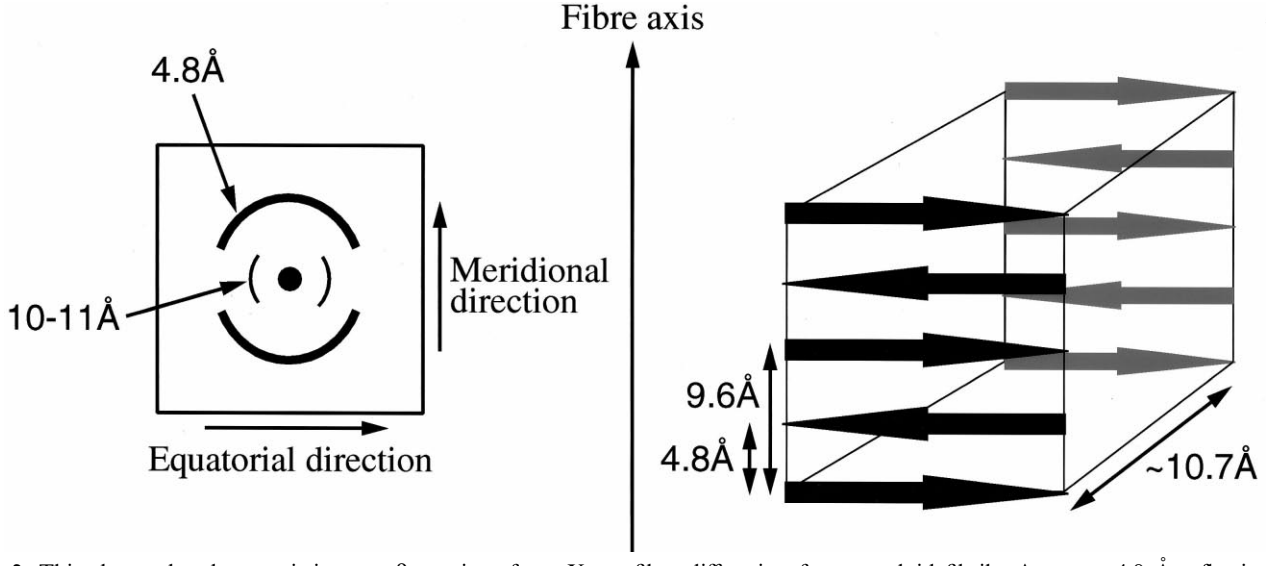

Fig. 2. This shows the characteristic cross-β spacings from X-ray fibre diffraction from amyloid fibrils. A strong 4.8 Å reflection on the meridian corresponds to the hydrogen bonding distance between β-strands (shown right), and a more diffuse 10–11 Å reflection on the equator shows the intersheet distance of about 10.7 Å. A spacing of 9.6 Å would correspond to the repeat distance for an anti-parallel arrangement of β-strands. This is not always observed in poorly aligned diffraction patterns, but often in well aligned patterns [34].

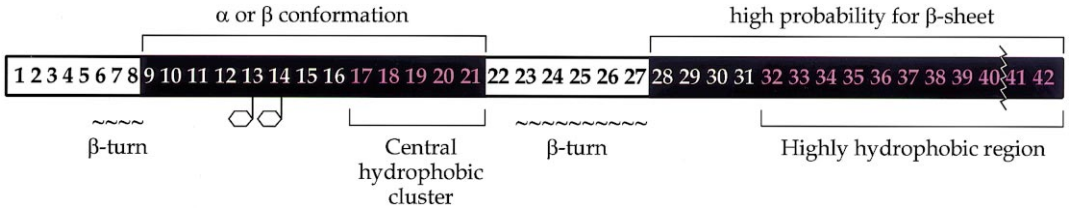

Fig. 3. This figure shows the results of structure prediction [13,14] which suggests regions with a high propensity for β-sheet structure, shown in black. Clusters of hydrophobic residues are shown in magenta.

have concentrated on using NMR, CD and FTIR methods to look at the structure of different regions of Aβ in various solvents. Atomic force microscopy (AFM) has proved a valuable tool to investigate the nature of the intermediates in the amyloid pathway. Transmission EM and fibre diffraction have been used to examine the structure of the amyloid fibrils, as well as methods of solid state NMR and FTIR. Fascinating work on the amyloid plaques themselves using optical microscopy reveals much about how the fibrils must assemble in vivo. Here I will concentrate on the structural aspects of amyloid fibril assembly and deposition. Although there is much to learn about amyloid structure from studies of other amyloid diseases, this review will only touch on those studies (see [2,12]).

2. The structure of soluble Aβ

Structure prediction studies [13] have indicated that the C-terminal 10 residues and residues 17–21 of Aβ show the greatest hydrophobicity while the C-terminus (from residue 28) showed a high probability for β-sheet structure. Residues 9–21 showed a lower probability for β-sheet. Two β-turns are predicted between residues 6 and 8, and residues 23 and 27 [13,14]. These characteristics are highlighted in Fig. 3.

The structure of the Aβ peptide has been extensively studied in solution, although it is necessary to use organic solvents such as DMSO and TFE, and detergents such as SDS to keep Aβ soluble. The results of many experiments on various length fragments homologous to Aβ are summarised in Table 1. NMR, CD and FTIR studies have shown that Aβ generally forms α-helical conformation in organic solvents [15,16,18–20,22,23,25,29,31–33,35] whereas in aqueous buffers or in water it is predominantly β-sheet, although this can be affected by pH, concentration and incubation time [9,11,36]. Detailed NMR studies of Aβ1–40 in 'membrane mimicking' solvents have revealed the existence of helices between residues 15 and 36 [31] or 35 [33], with a 'kink' at residues 25–27 [31] or loop at 24–30 [33]. Another study showed Aβ1–40 and 1–42 containing helices at 10–24 and 28–42 [35]. The difference in these results can be attributed to differences in pH and solvent (see Table 1). Similar studies on shorter peptides also show disordered residues at 25–27 [19,20,23].

3. Conformational switching

Aβ β-sheet content is linked to insolubility [10] and related to neurotoxicity [9]. The fibrillar state has also been shown to be associated with protease resistance [38]. It is thought that the Aβ peptide undergoes a conformation switch from α-helical to β-sheet structure during amyloidogenesis and that the structures of Aβ examined in organic 'membrane mimicking' solvents resemble the structure of Aβ in vivo [16,35]. Regions of the Aβ peptide responsible for conformational switching and fibrillogenesis have been examined using solvents at various pHs to look at the effect of ionisation on side chains, amino acid substitutions and truncation of Aβ from either the N- or C-terminus.

The N-terminus is thought to be important for initiating α–β conformational switching. An α-helix in Aβ1–28 was shown to unfold with increasing temperature and at mid-range pH and the hydrophobic residues within 13–20 unfold under these conditions [16]. A mechanism for the α-helix (monomer) to β-sheet (oligomer) transition may involve the deprotonation of side chains Asp7, Glu11, Glu22 and Asp23 above pH 4 and the protonation of His6, 13 and 14, causing a destabilisation of the α-helix [16].

Table 1

Region of Aβ	Method	Solvent and conditions	Structure/conformation	Reference
1–28	CD	water (pH 1–4)	random coil	[15]
1–28	NMR	TFE (pH 1–4)	α-helix; increased temperature leads to decrease in helix, 13–20 remain most stable helix	[15,16]
1–28	CD	water (pH 4–7)	β-sheet	[16]
1–28	NMR	water (pH 5.6)	not α-helical, extended strand	[17]
1–28	NMR	membrane mimic, SDS and TFE	α-helix, bend at 12	[18]
1–28 and 1–28 (E22Q)	NMR	DMSO	C-terminal α-helix, N-terminal turn (flexible)	[19]
1–28	EM, FD	aqueous	fibrillar, cross-β	[14]
1–28 (K16A)	EM, FD	aqueous	amorphous, cross-β	[14]
12–28	NMR	SDS (pH 5.6)	α-helix 16–24	[20]
x–28 (19–28, 17–28, 15–28, 13–28, 9–28)	FTIR, FD	various pH (aqueous)	β-sheet dependent on pH (most β-structure at ∼pH 3–7); 19–28 showed low β and mostly random coil	[8]
10–23	FTIR	solid state	β-sheet (antiparallel)	[11]
10–24	FTIR, CD	unclear	α-helix	[13]
10–24	FTIR, CD	unclear	β-sheet	[13]
10–35	ssNMR	dried from water (pH 7.4)	β-sheet (parallel)	[21]
19–35, 25–35 (Met35 analogues)	CD	various (aqueous, increased pH; ACN; TFE)	increased β-sheet structure with time from random coil; α-helix in TFE	[22]
25–35	NMR	LiDS and TFE (pH 4)	α-helix 28–34, disordered 25–27	[23]
25–35	CD	aqueous (pH 4, 5)	β-sheet > random coil (decreased concentration)	[24]
		(pH 5.5)	β-sheet	
		(pH 7.4)	β-sheet	
25–35	CD, FTIR	TFE	β-sheet	[25]
26–33	FTIR	water	random coil or α-helix	[10]
29–42	FTIR	solid state	β-sheet (antiparallel)	[11]
29–42	CD	aqueous (pH 7.4)	β-sheet	[11]
34–42	ssNMR	aqueous	β-sheet (antiparallel)	[26]
34–42	FTIR	water	β-sheet	[26]
1–39	CD	aqueous (pH 7.3)	random coil and β-sheet	[15]
1–39	CD	TFE (30%) (pH 1–4, 7–10)	α-helix	[15]
1–39	FTIR	DMSO (100%)	no β-sheet content	[27]
1–39	CD	aqueous (pH 7.4)	β-sheet (∼60%)	[27]
1–39	CD	TFA (0.1%) (pH 7.4)	β-sheet (∼30%)	[28]
1–39	CD	ACN (35%)/TFA (0.1%)	β-sheet (∼60%)	[28]
1–40	FTIR	aqueous (pH 7.5)	'1% α, 60% β', mostly β-sheet	[29]
1–40	CD	TFE (20%) (pH 7.4)	'16%' α-helix	[29]
1–40 (V18A)	FTIR	aqueous (pH 7.5)	'33% α, 31% β', α-helix and β-sheet	[29]
1–40 (V18A)	CD	TFE (20%) (pH 7.4)	'50% ' α-helix	[29]
1–40 (E22Q)	CD	TFE (20%) (pH 7.4)	'6%' α-helix	[29]
1–40	CD	aqueous (pH 7.8)	β-sheet (∼55%)	[30]
1–40	NMR	SDS (pH 5.1)	α-helix 15–36, kink 25–27	[31]
1–40 Met35Ox	NMR	SDS (pH 5.3)	α-helix 16–24	[32]
1–40	NMR	TFE (40%) (pH 2.8)	α-helix 15–23, 31–35	[33]
1–40	FD	water	cross-β	[34]
1–42	CD	water	β-sheet	[15]
1–42	CD	TFE (30%) (pH 1–4, 7–10)	α-helix	[15]
1–40 and 1–42	NMR	(SDS) (pH 7.2)	α-helix 10–24 and 28–42	[35]
10–43	CD	water	'80%' β-sheet	[11]
10–43	CD	HFIP	'28%' α-helix	[11]
ex vivo	FD	water extracted	cross-β	[37]

At a critical concentration, this may be accompanied by rearrangement to an oligomeric β-sheet [16]. Fibril formation studies of Aβx–28 (see Table 1) in various pH environments [8] revealed the importance of electrostatic interactions involving His–Asp/Glu salt bridges as well as hydrophobic contacts in the region Leu17–Ala21 and a model is proposed by which a central intersheet core of electrostatic and hydrophobic interactions stabilises an anti-parallel arrangement of β-strands defined by residues 13–23 [8,14]. NMR analysis of Aβ12–28 in water identified a central hydrophobic cluster at residues 17–21, but did not find evidence for salt bridge interactions between His14 and Glu22 [39].

Introduction of a single amino acid substitution (V18A) in Aβ1–40, which leads to an increased propensity for α-helical conformation compared to wild type, was found to be related to a decreased ability to form amyloid fibrils [29]. Substitution of residues Lys16 in Aβ1–28 [14] or Phe19 or 20 for Ala in 10–23 [11] results in peptides unable to form amyloid-like fibrils in vitro. It has also been observed that Aβ1–40 and Aβ1–42 with the Dutch-type amyloidosis mutation, Glu22Gln, show increased amyloid fibril formation and fibril stability compared to wild type [9,40,41]. This results from a decrease in electrostatic potential in the hydrophobic core region of 17–21 causing an enhancement of interactions between uncharged side chains [9].

Extensive studies of Aβ43 [11] and fragments of this peptide revealed that region 10–42 may form the β-sheet core of the amyloid fibrils, whereas residues 1–9 may be exposed on the surface of the fibres and be involved in interaction between fibrils. Truncated peptides from the Aβ N-terminus showed that residues 1–9 were not necessary for fibril formation [11]. The presence of a β-turn was mapped to residues 26–29 by protease digestion of various internally cross-linked peptides with engineered disulfides, and the flanking regions were proposed to form two β-strands. Fragments of 10–23 and 29–42 were both found to form β-sheet structure by FTIR, but 29–42 was less soluble and formed only very short fibrils, whereas 10–23 formed long fibrils. Recently, Norstedt and co-workers [42] showed that the smallest region of the N-terminus of Aβ capable of forming amyloid fibrils was residues 14–23, and that deletions or substitutions in this region result in the loss of fibril forming ability, suggesting that this sequence forms the core of Aβ fibrils.

4. Structure of Aβ fibril intermediates

Beta-sheet conformation is tightly linked to fibrillogenesis [43]. The kinetics of amyloid fibril assembly have been well studied and are discussed by Roher in this edition. It is thought that fibril formation proceeds via a nucleation dependent mechanism which is highly concentration dependent and that this proceeds via a partially folded intermediate [43]. Purification of Aβ1–42 peptide from Alzheimer's disease brain yielded stable dimeric and trimeric forms, and monomers which were then capable of forming fibrils in vitro [44]. Fluorescence spectroscopy and fluorescence resonance energy transfer of Aβ1–40 have shown that it is capable of existing as a stable dimer in aqueous solutions [45].

Examination of amyloid fibril formation from various synthetic peptides has revealed the presence of an intermediate in the pathway that has been visualised by EM, sedimentation and AFM. The first stage can be described as 'seeds' and these are usually described as being spherical or globular in appearance [46,47]. Sedimentation analyses identified aggregates of 50 000 S (around 10^{10} Da) and ∼30 S (around 10^6 Da) [48] and quasi-elastic light scattering (QLS) studies suggest that these may be represented by 'micelles' of Aβ [49] which have an estimated diameter of 140 Å. AFM in situ has suggested that the globular particles associate over time [47] and following fibril formation using QLS has inferred that monomers associated to form micelles from which fibrils nucleate and then elongate [49]. Studies of the short Aβ14–23 peptide suggest that fibril polymerisation [42] proceeds via the formation of dimers, then tetramers and finally oligomers, in which the charged residues form ion pairs and the hydrophobic residues form a hydrophobic core. This pathway for fibrillogenesis is supported by results from other groups for Aβ1–40 and 1–42 [50,51]. Although the structure of the intermediate is unknown, a theoretical model has been suggested based on the fact that Aβ1–42 shows some sequence homology to the enzymes catalase and triosephosphate isomerase. Both proteins are in an anti-parallel β-sheet conformation [52] and mod-

elling studies of Aβ have led to a proposed Greek key motif which dimerises to form a β-barrel arrangement exhibiting a hydrophobic core and a hydrophilic surface [52].

5. From 'protofibrils' to fibrils

'Protofibrils' have been described by a number of investigators [50,51,53]. These appear to be precursors to full-length fibrils, which have a curved appearance and are generally shorter than fully formed fibrils. Negative stain EM of protofibrils formed from Aβ1–40 and 1–42 show flexible fibres around 60–100 Å in diameter [53].

AFM has recently revealed more detailed information about the process of aggregation of the Aβ peptide. Small ordered aggregates or 'protofibrils' (∼30 Å diameter by 200–700 Å) were clearly observed at the early stages of fibril formation for both Aβ1–42 and Aβ1–40 [50]. These elongated with time and showed a beaded appearance and a periodic repeat of ∼220 Å. The protofibrils were closely followed by the appearance of longer fibrils of two different morphologies. 'Type 1' fibrils were around twice the diameter of the protofibrils (∼70–80 Å) and showed a periodic twist every ∼430 Å. Type 2 fibrils generally appeared later and were around 38–45 Å in diameter and did not show an obvious periodicity. Aβ42 fibrils formed more rapidly than Aβ40 fibrils. Stine et al. [53] also report the appearance of both smooth and periodic twisted fibrils of Aβ1–40 by AFM with thicknesses of about 40–60 Å or 80–120 Å respectively. They describe a periodicity of around 250 Å. Small protofibrils with an estimated diameter of 20–30 Å were also observed.

In situ AFM of Aβ1–42 aggregation upon hydrophilic mica or hydrophobic graphite has allowed the time course of fibril formation to be followed in phosphate-buffered saline [47] and shows a marked difference between the behaviour of Aβ on the two different environments. Small globular aggregates (∼50–60 Å height) were observed on the hydrophilic support, which tended to coalesce slowly over time, whereas on the hydrophobic support, Aβ aggregated to form narrow elongated sheets, which appeared to orient into parallel assemblies in line with the carbon atoms of the graphite support. The average lateral spacing was around 180 Å with a height of ∼10–12 Å, suggesting the formation of a single β-sheet which interacts with the hydrophobic surface. These data point to the importance of hydrophobic interactions between the β-sheets in amyloid fibrils.

6. Composition of fibrils – protofilaments

Cross-sections of synthetic Aβ amyloid fibrils (residues 11–28, 1–28 [8,14], 6–25 [7]) have been viewed by taking thin sections of embedded fibrils and examining them under the electron microscope. They appear to be composed of five or six protofilaments arranged around a 'hollow' centre, each protofilament having a diameter of around 25–30 Å. Interpretation of X-ray diffraction patterns from aligned fibrils of Aβ has also led to the conclusion that the fibrils are composed of five or six protofilaments (or subfibrils) [54]. The details of this are discussed in Section 7. Amyloid fibrils from other disease states have been examined by EM and these also suggest a packing of several protofilaments making up the amyloid fibril [4,55].

7. Beta-sheet structure of amyloid fibril protofilaments

Fibre diffraction and solid state NMR have revealed much about how the β-sheets are arranged within the amyloid fibril protofilament. Fibre diffraction data show only the repeating structure within a molecule. Beta-sheet structure along the fibre axis is shown up by the intense 4.7–8 Å reflection, since the hydrogen bonding of β-strands up the fibres extends infinitely. The length of the hydrogen bonds does not vary since it is sequence independent. Solid state NMR is capable of measuring interactions over relatively short ranges (∼6 Å), and therefore contributes information about the local interactions within the β-sheets. Both these methods describe the structure within the protofilament, although some limited information about protofilament packing can be revealed by fibre diffraction.

Fibre diffraction studies of ex vivo Aβ amyloid fibrils from Alzheimer's plaques showed an unoriented cross-β pattern with rings at 4.74 Å and 10–

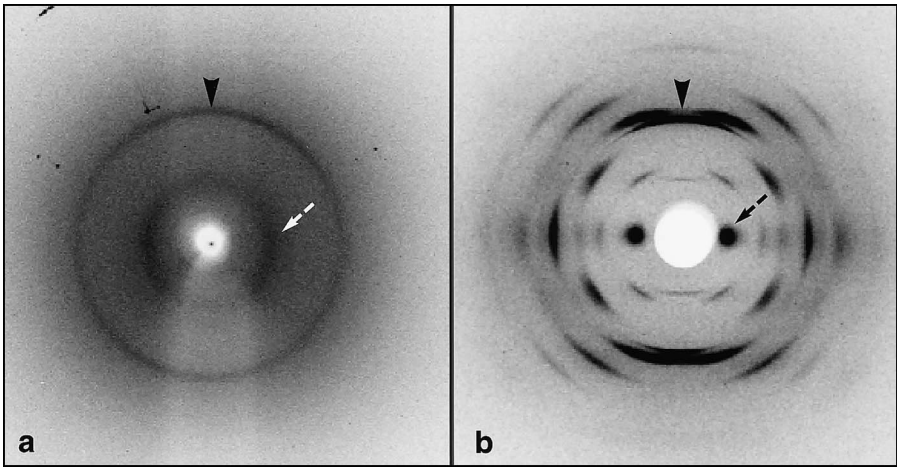

Fig. 4. X-ray fibre diffraction patterns of (a) a partially aligned sample of Aβ1–40 amyloid fibrils and (b) a magnetically aligned sample of Aβ11–25 amyloid fibrils. The small arrow shows 10–11 Å reflection on the equator and the arrowhead shows the strong 4.8 Å reflection on the meridian in both (a) and (b) (Serpell, unpublished).

11 Å which indicates a β-structure with the strands running perpendicular to the fibre axis [37]. This diffraction pattern has also been observed from various ex vivo amyloid fibrils [3], suggesting that amyloid fibrils composed of different proteins may share a common core structure. A structural model of the transthyretin amyloid fibril protofilament has been described as a β-sheet helix type structure with four β-sheets composed of β-strands running perpendicular to the fibre axis and turning around a central axis with a twist of 15° between one β-strand and its hydrogen bonded neighbour [56]. Improvement of the alignment of the amyloid fibrils by incubating synthetic Aβ peptides in a magnetic field revealed highly aligned diffraction patterns [54]. This method appears to work well for the orientation of smaller peptides which form amyloid fibrils whilst in the magnetic field, but less well for full-length Aβ peptides [34,54] or for ex vivo amyloid fibrils (Serpell, Sunde, Fraser, unpublished results). Fig. 4 shows X-ray fibre diffraction patterns from partially aligned Aβ1–40 fibrils and magnetically aligned Aβ11–25.

A model of the Alzheimer's amyloid fibre has been suggested from fibre diffraction of magnetically oriented samples and EM of Aβ1–40 [34]. Negative stain EM indicated that Aβ1–40 forms a mixture of twisted fibres (60–90 Å diameter and 460 Å pitch) and straight fibres (60–80 Å diameter). Thin sections of the fibrils suggested that they were composed of several protofilaments arranged around an electron lucent centre and the fibre diffraction pattern showed the characteristic cross-β pattern consisting of a sharp 4.7 Å meridional reflection and a broad reflection centred at 9 Å on the equator. The diffraction pattern also revealed lower angle reflections on the equator at 49.2 Å, 19 Å and 13.7 Å. The fibre pattern was interpreted to have arisen from a structure in which pairs of β-sheets (with a spacing of 9 Å between them) form a tubular cylinder of diameter ~28 Å, this comprises one protofilament, and between three and five protofilaments make up the ~70 Å fibril. It is suggested that the β-strands do not run perpendicular to the fibre axis as is generally interpreted from cross-β patterns [57,58], but that the strands are tilted by 35.6° [9,34]. This is inferred from a previous Aβ40 diffraction pattern [9] in which reflections at 4.7 Å and at 3.84 Å are both off meridional. However, Malinchik et al. [34] show that both reflections are meridional in their more recent Aβ40 pattern and attribute this to cylindrical averaging (see [59]). In previous fibre diffraction analyses of several different amyloid fibrils [3,56] the 3.84 Å off-meridional reflection was also noted and was attributed to the spacing between Cα in a pleated β-sheet being arranged in a helical manner. A further weak meridional spacing at around 54 Å [7], 53 Å [54] or 57 Å [9] on the Aβ1–40 diffraction pattern has been suggested to correspond to an axially repeating unit

consisting of ~12 hydrogen bonded β-strands (i.e. half number suggested for TTR [56]), but could also arise from a helical twist.

In a previous publication Kirschner and colleagues [54] presented an extensive library of fibre diffraction patterns from different length peptides of Aβ. The fibrils were aligned in a magnetic field and produced well-oriented diffraction patterns. The diffraction patterns could be separated into three groups.

The first group (residues 19–28, 13–28, 12–28, 11–28, 9–28, 1–28, 1–38, 1–40, 6–25, 11–25 and 34–42) exhibited patterns showing the characteristic cross-β reflections (see Fig. 4b). Some of these patterns were analysed and were assigned a monoclinic spacegroup and a cell of $a = 9.44$ Å (hydrogen bonding direction), $b = 6.92$ Å (polypeptide chain direction), $c = 10.76$ Å (intersheet spacing) which would contain two amino acid residues in a pleated-β conformation (see Fig. 5). Diffraction patterns from Aβ6–25 and Aβ11–28 showed sampling of Bragg reflections along layer lines suggesting a highly organised packing of fibres within the sample. Modelling of a possible structure of β-crystallites was attempted using phases from the structure of β-keratin (which is incidentally extended-β with strands running along the fibre axis, not cross-β [60]). The equatorial reflections were found to index to a one-dimensional lattice (~ 60 Å). This could be explained by either a cylindrical lattice or a restricted crystalline lattice. However, the model interpreted to best fit the Aβ11–28 data was a hollow cylinder or tube composed of five β-crystallites, each 20 Å by 50 Å. These were arranged in a pentamer with centres exactly positioned at lattice points. The crystallites (or 'subfibrils' = protofila-

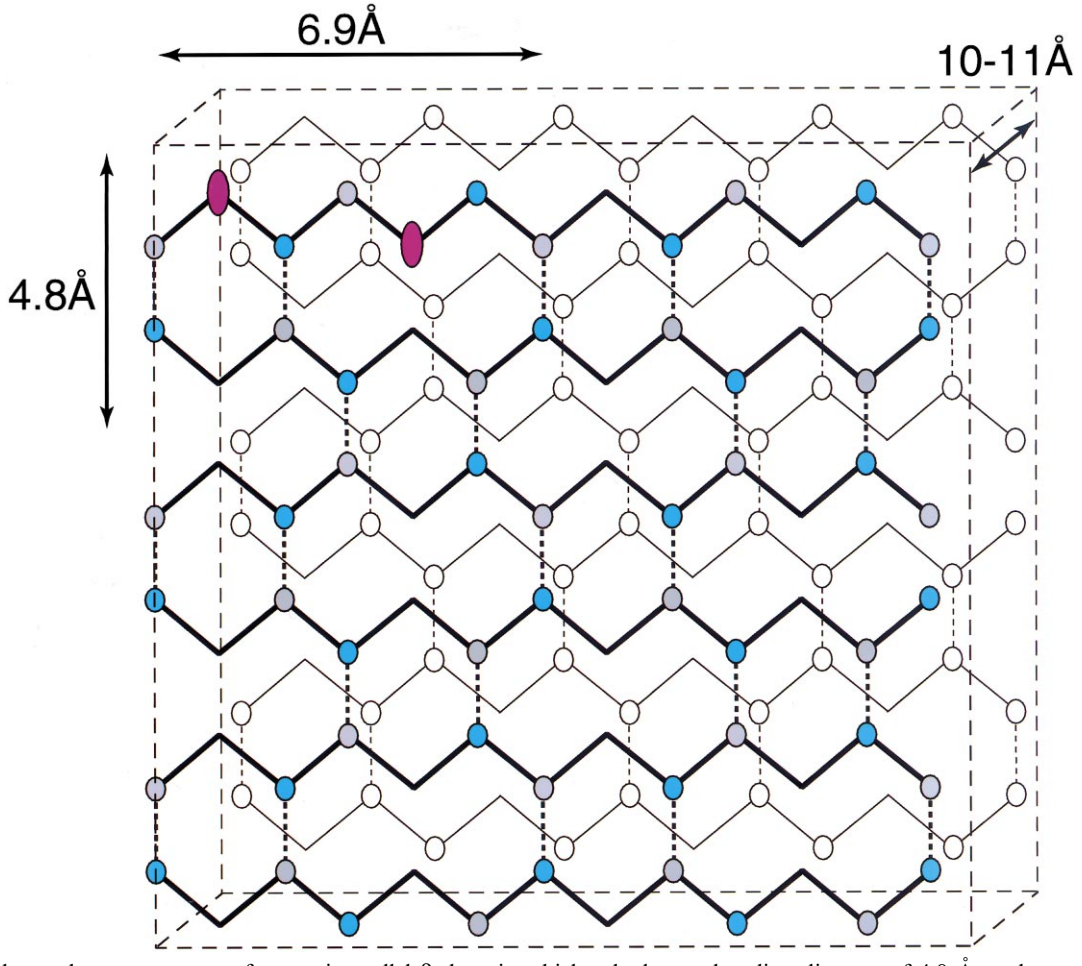

Fig. 5. This shows the arrangement of an anti-parallel β-sheet in which a hydrogen bonding distance of 4.8 Å, a sheet spacing of 10–11 Å and a repeat distance along the polypeptide chain of 6.9 Å are apparent.

ments) were thought to be made up of approximately five β-sheets (each with a spacing of 10 Å between them) and around six residues (three lattice points, 6.9 Å between every other Cα) along the polypeptide chain.

A second group (18–28, 17–28, 15–28) were thought to arise from a plate-like arrangement of β-sheets with the rotation axis parallel to the polypeptide chain. These structures were extended in both the hydrogen bonding and intersheet directions. The loss of His13 and His14 from these peptides as compared to many of those in group A may account for the difference in forming tubular or plate-like structures [54], suggesting that the histidines weaken, rather than strengthen the intersheet interactions (however, this is not clear cut, since 19–28 is in group A).

Finally, the third group (22–35, 26–33) resulted in fibre diffraction patterns with no alignment, likely to be due to disorientation of the β-crystallites.

The authors suggest that the hydrophobic residues Leu17-Val18-Phe19-Phe20 and Ala21 form the core interactions in the intersheet direction and that remaining ionic residues may be involved in interaction between 'subfibrils' or protofilaments.

This publication concentrated predominantly on the intersheet direction and did not discuss the hydrogen bonding direction. Whether or not these data indicate parallel or anti-parallel arrangement of β-strands is unclear [54]. The presence of a layer line at 9.4 Å is suggestive of an anti-parallel arrangement of β-strands, since this spacing would correspond to every other β-strand which would be the true repeat. However the reflection corresponding to the β-strand spacing 4.7 Å is by far the strongest in these diffraction patterns (see Fig. 4).

The structure of amyloid fibrils formed from Aβ10–35 has been studied using solid state NMR [21]. ^{13}C were positioned at Gln15 and Lys16, because of previously published results of cross-linking studies using transglutaminase which showed that Gln15 from one peptide and Lys16 from the next are adjacent in the amyloid fibril [61–65]. In Aβ10–35 ^{13}C Gln15, a distance measured between the ^{13}C from adjacent peptides was 5.1 Å (±0.2), and for Aβ10–35 1-^{13}C Lys16 4.9 Å (±0.2). These distances of around 5 Å could fit models of anti-parallel and parallel β-structure. However, the NMR data can be explained by a model in which every ^{13}C carbonyl interacts with two, equidistant ^{13}C carbonyls and these data are best fitted by a parallel arrangement in which the residues are in exact register. This interpretation was further validated by the measurement of 5.0 Å spacings for two new peptides containing ^{13}C carbonyls at residues 17 and 18, which can be most clearly explained by a parallel arrangement, since no interaction would be detected for an anti-parallel arrangement. However, this model is difficult to fit to previously observed characteristics. FTIR measurements have consistently referred to anti-parallel structure for Aβ amyloid [10,11]. Fibre diffraction studies of fibrils formed from various fragments of Aβ have found layer lines corresponding to a 9.6 Å repeating unit [7–9,34,54] which is thought to arise from an anti-parallel arrangement with the repeat being every other β-strand. Benzinger et al. [21] do not account for the rest of the Aβ10–35 in their model of the parallel β-strand arrangement (only the six residues 13–18) and it is difficult to understand how the remaining structure would fold into a β-sheet without allowing for β-hairpin formation and therefore anti-parallel β-sheet conformation. If β-strands were in an extended β-strand conformation then they would measure around 6.95 Å [66] × 42/2 = 146 Å for Aβ1–42 and 139 Å for Aβ40, which is larger than the 40–80 Å measurement of fibrils formed in vitro [14,50,53]. A structural model of amyloid fibrils formed from Aβ34–42 [26] using solid state NMR rejected the possibility of β-hairpins making up the structure based on searching a library of conformations against the data. They suggest that the fibrils were made up of extended β-strands in an anti-parallel arrangement. One possibility for a parallel β-sheet arrangement is suggested by a β-helix type structure [67–72]. This type of structure has been suggested for amyloid by Lazo and Downing [73], although more rigorous model building and measurements of spacings are necessary to ensure that the model will fit with experimental data [3,14,37] before any conclusions can be drawn about the validity of this theoretical model. Another possibility could be an arrangement with a mixture of parallel and anti-parallel β-hairpins as shown in Fig. 6.

A study by O'Chaney et al. [52] suggested a theoretical three-dimensional model of the Aβ1–42 amy-

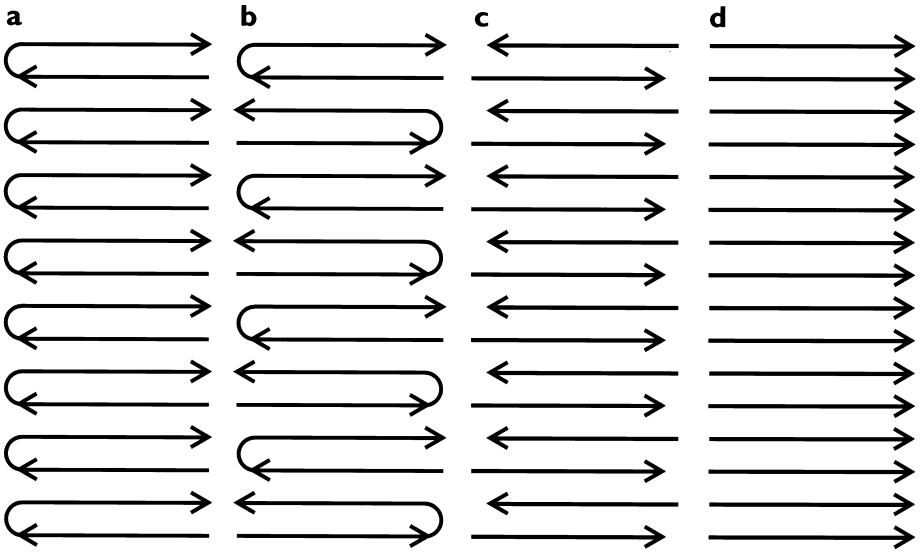

Fig. 6. Four possible arrangements for a short β-strand (e.g. 10–35 [21], 34–42 [26]. (a) anti-parallel β-hairpin arrangement; (b) theoretical anti-parallel β-hairpins arranged parallel to one another; (c and d) extended β-strands in anti-parallel (c) and parallel (d) arrangements.

loid fibril. This was built from tetrameric building blocks consisting of two 'β-barrel' dimers with C-terminal domain (residues 30–42) extended to form an anti-parallel β-sheet [52]. These were then further dimerised to form an octamer consisting of hydrophobic twisted β-sheet (C-terminal domains of Aβ1–42 monomers) flanked by a series of adjacent β-barrels arranged helically around the sheet. This model is proposed to comprise the protofilament (diameter ~65 Å). It was then suggested that three of these protofilaments intertwine to form the fibril (diameter ~120 Å) forming structure which appears to be composed of six globular units (three dimers) in cross-section [52].

8. Amyloid fibril deposition and structure of the plaques in Alzheimer's disease

Amyloid fibrils are deposited in neuritic plaques extracellularly in the cortex of Alzheimer's disease brains. The central deposit of amyloid fibrils (the core) is surrounded by dystrophic neurites, activated microglia and reactive astrocytes.

Studies of the morphological structure of the senile plaque using optical microscopy [74] have revealed that they typically consist of a porous core with characteristic pore sizes and a diffuse ring from which the density decays from the centre of mass of the core. The authors propose that this pattern of structure could be produced from a process whereby aggregation occurs simultaneously with disaggregation thus producing a porous structure. This model would explain the observation that the amount of Aβ deposited in patients varies only slightly and does not increase with disease progression, but remains relatively constant [74].

The molecular structure of the plaques has been studied in situ using FTIR microspectroscopy methods [75], and this has shown that the core of the plaques gives a strong β-sheet conformation signal compared to an α-helical or random signal from surrounding areas of grey matter. The observation of β-sheet is consistent with results from biophysical methods from ex vivo and synthetic amyloid [14, 37].

9. Alzheimer's disease amyloid associated molecules

In vivo the concentration of Aβ is much less than is used in fibril formation in vitro. It is thought that other proteins and molecules play an important role in amyloid fibril formation and deposition. These

will be mentioned briefly. They include the glycosaminoglycan (GAG), heparan sulfate proteoglycan (HSPG) [76], serum amyloid P (SAP) [77], apolipoprotein E (Apo E) [78,79], α1-antichymotrypsin (ACT) [80] and complement factors (C1q, C3d and C4d [81]).

HSPG is associated with amyloid fibrils in all amyloid diseases and is thought to play an important role in amyloid deposition. GAGs can increase fibril formation and lateral aggregation of Aβ peptides in vitro [82]. The binding is thought to occur via sulfate groups, since addition of sulfate ions to peptides in vitro appears to show a similar effect. Fibre diffraction patterns of synthetic amyloid fibrils suggest a periodicity of 65 Å for sulfate binding along the fibre axis [82]. The effect of GAGs on fibril formation appears to be pH dependent [83] so the interaction of GAGs with amyloid proteins is thought to be via electrostatic interactions and in the case of Aβ is probably mediated by His13 and His14 [82].

SAP is also found in all amyloid deposits [77] and binds to them in a calcium dependent manner [84]. It is a member of the pentraxin family of proteins and exists as a decamer with two pentameric rings arranged face to face. Each subunit displays a jelly-roll fold of highly β-sheet structure [85]. SAP is highly protease resistant in the presence of calcium and is thought to have a role in protecting amyloid fibrils against degradation [86,87].

Apo E has been linked to some cases of late onset Alzheimer's disease [78,88] and is present in senile plaques. Unlike other amyloid associated proteins, ACT is specific to Alzheimer's disease. It co-localises with senile plaques and vascular amyloid during the earliest stages of its development [80,89]. ACT is a member of the serine protease inhibitor family (serpins). Similarity between the Aβ residues Asp7-Ser8-Gly9 and active sites of serine proteases has led to the proposed ACT binding site [90]. ACT has been shown to have an effect on amyloid fibril formation [90,91].

10. Conclusions

Structural studies of amyloid fibrils are non-trivial. They are extremely insoluble and stable and therefore very difficult to work with by conventional methods. Aβ research has concentrated on the use of model peptides for structural studies, and this

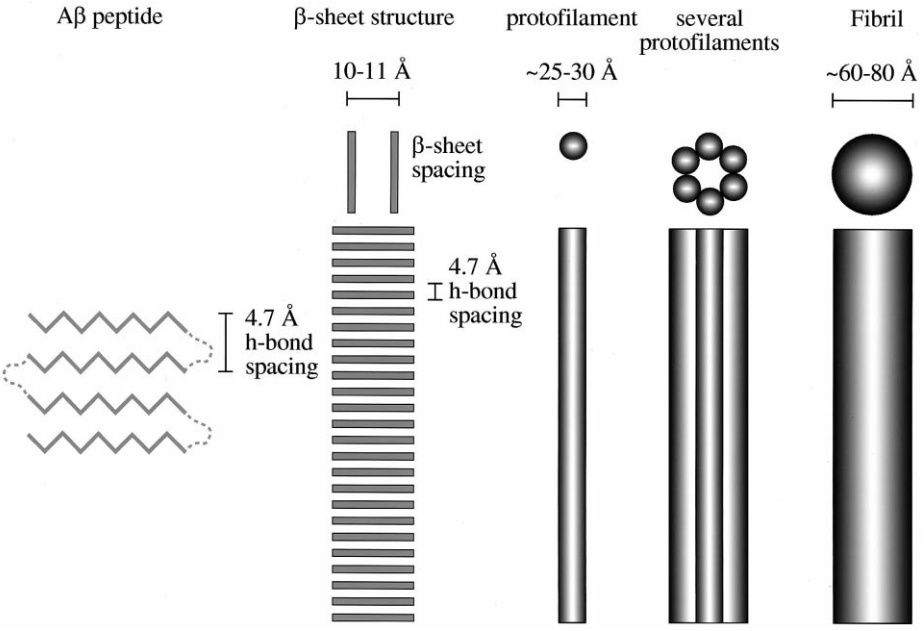

Fig. 7. This figure shows the hierarchy of structure from the Aβ peptide folded into a β-pleated sheet structure through protofilaments to amyloid fibrils. Views shown looking down the axis of the fibre and axially.

has led to an in-depth knowledge of the importance of various regions of Aβ. However, the information gathered from these studies is complex because of the many different solvents and conditions used in different studies of amyloid fibril structure and assembly.

In summary, studies of the Aβ peptide in various 'membrane mimicking' solvents had suggested α-helical conformation for the soluble Aβ peptide, whilst fibrillogenesis of Aβ has been shown to be linked to a conversion to β-sheet structure. Residues 11–16 are thought to be important in forming electrostatic interactions and residues 17–21 in hydrophobic interactions. A short peptide 14–23 is capable of forming amyloid fibrils in vitro and the region 11–24 is thought to play an important role in α to β conversion. Residues 25–35 have been implicated in neurotoxicity and residues 34–42 are very hydrophobic and are thought to be situated in the transmembrane region in APP. Peptides of this region are extremely insoluble and have been implicated in nucleating amyloid fibril formation.

Assembly of amyloid fibrils appears to be a complicated process which is still poorly understood. Whilst it is clear that amyloid fibrils are composed of several protofilaments (five or six), the mechanism of assembly and the exact morphology remain unclear. Protofibrils have been identified which appear to be fibrillar precursors to amyloid fibril formation, and these are preceded by the appearance of small oligomers of Aβ. Whether these small intermediates interact directly to form protofibrils and then these elongate to form the fully formed fibril, or whether protofilaments are formed first and then associate together remains ambiguous. The hierarchy of structures within amyloid fibrils are illustrated in Fig. 7.

The predominantly β-sheet structure of the protofilaments seems to be generally accepted, with β-strands running perpendicular to the fibre axis and held together by hydrogen bonding. Whether these are arranged parallel or anti-parallel is still under dispute and how these β-sheets assemble into the protofilament and then the fibril has been modelled, but not proven. Developing techniques for directly visualising amyloid fibrils at high resolution, such as cryo-electron microscopy with image processing and AFM combined with X-ray diffraction data and solid state NMR, may hold the key to solving the structure of the Alzheimer's amyloid fibril.

Acknowledgements

Thanks to Drs Aidan Doherty and Margaret Sunde for critically reading the manuscript. L.C.S. is funded by the MRC.

References

[1] D.J. Selkoe, The molecular pathology of Alzheimer's disease, Neuron 6 (1991) 487–498.
[2] M. Sunde, C. Blake, From the globular to the fibrous state: protein structure and structural conversion in amyloid formation, Q. Rev. Biophys. 31 (1998) 1–39.
[3] M. Sunde, L. Serpell, M. Bartlam, P. Fraser, M. Pepys, C. Blake, Common core structure of amyloid fibrils by synchrotron X-ray diffraction, J. Mol. Biol. 273 (1997) 729–739.
[4] T. Shirahama, A.S. Cohen, High resolution electron microscopic analysis of the amyloid fibril, J. Cell Biol. 33 (1967) 679–706.
[5] A.S. Cohen, T. Shirahama, M. Skinner, Electron microscopy of amyloid, in: I.R. Harris (Ed.), Electron Microscopy of Protein, 1982, Academic Press, London, pp. 165–205.
[6] E.D. Eanes, G.G. Glenner, X-ray diffraction studies on amyloid filaments, J. Histochem. Cytochem. 16 (1968) 673–677.
[7] P. Fraser, L. Duffy, M. O'Malley, J. Nguyen, H. Inouye, D. Kirschner, Morphology and antibody recognition of synthetic β-amyloid peptides, J. Neurosci. Res. 28 (1991) 474–485.
[8] P.E. Fraser, J.T. Nguyen, W.K. Surewicz, D.A. Kirschner, pH dependent structural transitions of Alzheimers amyloid peptides, Biophys. J. 60 (1991) 1190–1201.
[9] P.E. Fraser, J.T. Nguyen, H. Inouye, W.K. Surewicz, D.J. Selkoe, M.B. Podlisny, D.A. Kirschner, Fibril formation by primate, rodent and Dutch-hemorrhagic analogues of Alzheimer amyloid β-protein, Biochemistry 31 (1992) 10716–10723.
[10] K. Halverson, P. Fraser, D. Kirschner, P. Lansbury, Molecular determinants of amyloid deposition in Alzheimers disease: Conformational studies of synthetic β-protein fragments, Biochemistry 29 (1990) 2639–2644.
[11] C. Hilbich, B. Kisters-Woike, J. Reed, C. Masters, K. Beyreuther, Aggregation and secondary structure of synthetic amyloid βA4 peptides of Alzheimer's disease, J. Mol. Biol. 218 (1991) 149–163.
[12] L. Serpell, M. Sunde, C. Blake, The molecular basis of amyloidosis, Cell. Mol. Life Sci. 53 (1997) 871–887.
[13] C. Soto, M. Branes, J. Alvarez, N. Inestrosa, Structural determinants of the Alzheimer's amyloid beta-peptide, J. Neurol. Chem. 63 (1994) 1191–1198.
[14] D. Kirschner, H. Inouye, L. Duffy, A. Sinclair, M. Lind, D. Selkoe, Synthetic peptide homologous to β-protein from Alzheimer's disease forms amyloid-like fibrils in vitro, Proc. Natl. Acad. Sci. USA 84 (1987) 6953–6957.
[15] C.J. Barrow, M.G. Zagorski, Solution structures of β-pep-

tide and its constituent fragments relation to amyloid deposition, Science 253 (1991) 179–182.
[16] M. Zagorski, C. Barrow, NMR studies of amyloid β-peptide: Proton assignments, secondary structure and mechanism of an α-helix-β-sheet conversion for a homologous, 28 residue, N-terminal fragment, Biochemistry 31 (1992) 5621–5631.
[17] J. Lee, E. Stimson, J. Ghilardi, P. Mantyh, Y.-A. Lu, A. Felix, W. Llanos, A. Behbin, M. Cummings, M. Van Criekinge, W. Timms, J. Maggio, ^{1}H NMR of Aβ amyloid peptide congeners in water solution. Conformation changes with plaque competence, Biochemistry 34 (1995) 5191–5200.
[18] J. Talafous, K. Marcinowski, G. Klopman, M. Zagorski, Solution structure of residues 1–28 of the amyloid β-peptide, Biochemistry 33 (1994) 7788–7796.
[19] K. Sorimachi, D. Craik, Structure determination of extracellular fragments of amyloid proteins involved in Alzheimer's disease and Dutch-type hereditary cerebral haemorrhage with amyloidosis, Eur. J. Biochem. 219 (1994) 237–251.
[20] F. Fletcher, D. Keire, The interaction of β-amyloid protein fragment (12–28) with lipid environments, Protein Sci. 6 (1997) 666–675.
[21] T. Benzinger, D. Gregory, T. Burkoth, H. Miller-Auer, D. Lynn, R. Botto, S. Meredith, Propagating structure of Alzheimer's β-amyloid (10–35) is parallel β-sheet with residues in exact register, Proc. Natl. Acad. Sci. USA 95 (1998) 13407–13412.
[22] O. ElAgnaf, D. Guthrie, D. Walsh, G. Irvine, The influence of the central region containing residues 19–25 on the aggregation properties and secondary structure of Alzheimer's β-amyloid peptide, Eur. J. Biochem. 256 (1998) 560–569.
[23] T. Kohno, K. Kobayashi, T. Maeda, K. Sato, A. Takashima, Three-dimensional structures of the amyloid β peptide (25–35) in membrane-mimicking environment, Biochemistry 35 (1996) 16094–16104.
[24] E. Terzi, G. Holzemann, J. Seelig, Alzheimer β-amyloid peptide 25–35: Electrostatic interactions with phospholipid membranes, Biochemistry 33 (1994) 7434–7441.
[25] I. Laczko, S. Holly, Z. Konya, K. Soos, J. Varga, M. Hollosi, B. Penke, Conformational mapping of amyloid peptides from the putative neurotoxic 25–35 region, Biochem. Biophys. Res. Commun. 205 (1994) 120–126.
[26] P. Lansbury, P. Costa, J. Griffiths, E. Simon, M. Auger, K. Halverson, D. Kocisko, Z. Hendsch, T. Ashburn, R. Spencer, B. Tidor, R. Griffin, Structural model for the β-amyloid fibril based on interstrand alignment of an antiparallel-sheet comprising a C-terminal peptide, Nature Struct. Biol. 2 (1995) 990–998.
[27] C.-L. Shen, R.M. Murphy, Solvent effects on self assemply of β-amyloid peptide, Biophys. J. 69 (1995) 640–651.
[28] C.-L. Shen, M. Fitzgerald, R. Murphy, Effect of acid predissolution on fibril size and fibril flexibility of synthetic β-amyloid peptide, Biophys. J. 67 (1994) 1238–1245.
[29] C. Soto, E. Castano, B. Frangione, N. Inestrosa, The α-helical to β-sheet transition in the amino-terminal fragment of the amyloid β-peptide modulates amyloid formation, J. Biol. Chem. 270 (1995) 3063–3067.
[30] S. Tomski, R. Murphy, Kinetics of aggregation of synthetic β-amyloid peptide, Arch. Biochem. Biophys. 294 (1992) 630–638.
[31] M. Coles, W. Bicknell, A. Watson, D. Fairlie, D. Craik, Solution structure amyloid β-peptide (1–40) in a water-micelle environment. Is the membrane-spanning domain where we think it is?, Biochemistry 37 (1998) 11064–11077.
[32] A. Watson, D. Fairlie, D. Craik, Solution structure of methionine-oxidized amyloid β-peptide (1–40). Does oxidaton affect conformational switching?, Biochemistry 37 (1998) 12700–12706.
[33] H. Sticht, P. Bayer, D. Willbold, S. Dames, C. Hilbich, K. Beyreuther, R. Frank, P. Rosch, Structure of amyloid A4(1–40)-peptide of Alzheimer's disease, Eur. J. Biochem. 233 (1995) 293–298.
[34] S.B. Malinchik, H. Inouye, K. Szumowski, D. Kirschner, Structural analysis of Alzheimer's β(1–40) amyloid: protofilament assembly of tubular fibrils, Biophys. J. 74 (1998) 537–545.
[35] H. Shao, S. Jao, J. Ma, M. Zagorski, Solution structures of micelle-bound amyloid β-(1–40) and β-(1–42) peptides of Alzheimer's disease, J. Mol. Biol. 285 (1999) 755–773.
[36] S. Wood, B. Maleeff, T. Hart, R. Wetzel, Physical, morphological and functional differences between pH 5.8 and 7.4 aggregates of the Alzheimer's amyloid peptide Aβ, J. Mol. Biol. 256 (1996) 870–877.
[37] D. Kirschner, C. Abraham, D. Selkoe, X-ray diffraction from intraneuronal paired helical filaments and extra-neuronal amyloid fibres in Alzheimers disease indicates cross β conformation, Proc. Natl. Acad. Sci. USA 83 (1986) 503–507.
[38] C. Norstedt, J. Naslund, L. Tjernberg, A. Karlstrom, J. Thyberg, L. Terenius, The Alzheimer Aβ peptide develops protease resistance in associaction with its polymerization into fibrils, J. Biol. Chem. 269 (1994) 30773–30776.
[39] S. Zhang, N. Casey, J. Lee, Residual structure in the Alzheimer's disease peptide: probing the origin of a central hydrophobic cluster, Folding Design 3 (1998) 413–422.
[40] E. Levy, M. Carman, I. Fernadez-Madrid, I. Lieberburg, M. Poser, S. Van Duinen, G. Bots, W. Luyendijk, B. Frangione, Mutation of the Alzheimers disease gene in hereditary cerebral haemorrhage, Dutch type, Science 248 (1990) 1124–1126.
[41] T. Wisniewski, J. Ghiso, B. Frangione, Peptides homologous to the amyloid protein of Alzheimers disease containing glutamine for a glutamic acid substitution have accelerated amyloid fibril formation, Biochem. Biophys. Res. Coomun. 179 (1991) 1247–1254.
[42] L. Tjernberg, D. Callaway, A. Tjernberg, S. Hahne, C. Lilliehook, L. Terenius, J. Thyberg, C. Norstedt, A molecular model of Alzheimer's amyloid-β peptide fibril formation, J. Biol. Chem. 274 (1999) 12619–12625.
[43] P. Lansbury, Evolution of amyloid: what normal protein

folding may tell us about fibrillogenesis and disease, Proc. Natl. Acad. Sci. USA 96 (1999) 3342–3344.
[44] A.E. Roher, M. O'Chaney, Y. Kuo, S.D. Webster, W.B. Stine, L.J. Haverkams, A.S. Woods, R.J. Cotter, J.M. Tuohy, G.A. Krafft, B.S. Bonnell, M.R. Emmerling, Morphology and toxicity of Aβ-(1–42) dimer derived from neuritic and vascular amyloid deposits of Alzheimer's disease, J. Biol. Chem. 271 (1996) 20631–20635.
[45] W. Garzon-Rodriguez, M. Sepulveda-Becerra, S. Milton, C. Glabe, Soluble amyloid Aβ-(1–40) exists as a stable dimer at low concentrations, J. Biol. Chem. 272 (1997) 21037–21044.
[46] B. Seilheimer, B. Bohrmann, L. Bondolfi, F. Muller, D. Stuber, H. Dobeli, The toxicity of the Alzheimer's β-amyoid peptide correlates with a distinct fiber morphology, J. Struct. Biol. 119 (1997) 59–71.
[47] T. Kowalewski, D. Holtzman, In situ atomic force microscopy study of Alzheimer's β-amyloid peptide on different substrates: New insights into mechanism of β-sheet formation, Proc. Natl. Acad. Sci. USA 96 (1999) 3688–3693.
[48] S. Snyder, U. Ladror, W. Wade, G. Wang, L. Barrett, E. Matayoshi, H. Huffaker, G. Kafft, T. Holzman, Amyloid-β aggregation: selective inhibition of aggregation in mixtures of amyloid with different chain lengths, Biophys. J. 67 (1994) 1216–1228.
[49] A. Lomakin, D. Chung, G. Benedek, D. Kirschner, D. Teplow, On the nucleation and growth of amyloid β-protein fibrils: detection of nuclei and quantification of rate constants, Proc. Natl. Acad. Sci. USA 93 (1996) 1125–1129.
[50] J. Harper, S. Wong, C. Lieber, P. Lansbury, Observation of metastable Aβ amyloid protofibrils by atomic force microscopy, Chem. Biol. 6 (1997) 119–125.
[51] D. Walsh, A. Lomakin, G. Benedek, M. Condron, D. Teplow, Amyloid β-protein fibrillogenesis, J. Biol. Chem. 272 (1997) 22364–22372.
[52] M.O. Chaney, S. Webster, Y. Kuo, A. Roher, Molecular modelling of the Aβ1–42 peptide from Alzheimer's disease, Protein Eng. 11 (1998) 761–767.
[53] W. Stine, S. Snyder, U. Ladror, W. Wade, M. Miller, T. Perun, T. Holzman, G. Krafft, The nanometer-scale structure of amyloid-β visualized by atomic force microscopy, J. Protein Chem. 15 (1996) 193–203.
[54] H. Inouye, P. Fraser, D. Kirschner, Structure of β-crystallite assemblies by Alzheimer β amyloid protein analogues: Analysis by X-ray diffraction, Biophys. J. 64 (1993) 502–519.
[55] L. Serpell, M. Sunde, P. Fraser, P.K. Luther, E. Morris, O. Sandgren, E. Lundgren, C. Blake, The examination of the structure of the transthyretin amyloid fibril by image reconstruction from electron micrographs, J. Mol. Biol. 254 (1995) 113–118.
[56] C. Blake, L. Serpell, Synchrotron X-ray studies suggest that the core of the transthyretin amyloid fibril is a continuous β-helix, Structure 4 (1996) 989–998.
[57] A.J. Geddes, K.D. Parker, E.D.T. Atkins, E. Beighton, 'Cross β' conformation in protein, J. Mol. Biol. 32 (1968) 343–358.
[58] L. Pauling, R. Corey, Two β-pleated sheet configurations of polypeptide chains involving both cis- and trans- amide groups, Proc. Natl. Acad. Sci. USA 39 (1953) 247–252.
[59] H. Inouye, X-ray-scattering from a discrete helix with cumulative angular and translational disorders, Acta Crystallogr. A. 50 (1994) 644–646.
[60] R. Fraser, T. MacRae, An investigation of the structure of β-keratin, J. Mol. Biol. 5 (1962) 457–466.
[61] D.J. Selkoe, C. Abraham, Y. Ihara, Brain transglutaminase – in vitro crosslinking of human neurofilament proteins into insoluble polymers, Proc. Natl. Acad. Sci. USA 79 (1982) 6070–6074.
[62] L. Rasmussen, E. Sorensen, T. Petersen, J. Gliemann, P. Jensen, Identification of glutamine and lysine residues in Alzheimer amyloid β-A4 peptide responsible for transglutaminase-catalyzed homopolymerization and cross-linking to alpha(2)M receptor, FEBS Lett. 338 (1994) 161–166.
[63] G. Ho, E. Gregory, I. Smirmova, M. Zoubine, B. Festoff, Cross-linking of β-amyloid protein precursor catalyzed by tissue transglutaminase, FEBS Lett. 349 (1994) 151–154.
[64] S. Dudek, G. Johnson, Transglutaminase facilitates the formation of polymers of the β-amyloid peptide, Brain Res. 651 (1994) 129–133.
[65] K. Ikura, K. Takahata, R. Sasaki, Cross-linking of a synthetic partial-length (1–28) peptide of the Alzheimer β/A4 amyloid protein by transglutaminase, FEBS Lett. 349 (1993) 109–111.
[66] R.E. Marsh, R.B. Corey, L. Pauling, Biochim. Biophys. Acta 16 (1955) 1–34.
[67] M. Yoder, S. Lietzke, F. Jurnak, Unusual structural features in the parallel β-helix in pectate lyases, Structure 1 (1993) 241–251.
[68] M. Yoder, N. Keen, F. Jurnak, New domain motif – the structure of pectate lyase-C, a secreted plant virulence factor, Science 260 (1993) 1503–1506.
[69] M. Yoder, F. Jurnak, Protein motifs. 3. The parallel β-helix and other coiled folds, FASEB J. 9 (1995) 335–342.
[70] V. Sieber, F. Jurnak, G. Moe, Circular dichroism of the parallel β-helical proteins pectate lyase-C and lyase-E, Proteins Struct. Funct. Genet. 23 (1995) 32–37.
[71] S. Steinbacher, R. Seckley, D. Miller, B. Steipe, R. Huber, P. Reinemer, Crystal-structure of P22 tailspike protein – interdigitated subunits in a thermostable trimer, Science 265 (1994) 383–386.
[72] C. Raetz, S. Roderick, A left-handed parallel β-helix in the structure of UDP-*N*-acetylglucosamine acyltransferase, Science 270 (1995) 997–1000.
[73] N. Lazo, D. Downing, Amyloid fibrils may be assembled from β-helical protofibrils, Biochemistry 37 (1998) 1731–1735.
[74] L. Cruz, B. Urbanc, S. Buldyrev, R. Christie, T. Gomez-Isla, S. Havlin, M. McNamara, H. Stanleu, B. Hyman, Aggregation and disaggregation of senile plaques in Alzheimer's disease, Proc. Natl. Acad. Sci. USA 94 (1997) 7612–7616.
[75] L. Choo, D. Wetzel, W. Halliday, M. Jackson, S. LeVine, H. Mantsch, In situ characterization of β-amyloid in Alzheim-

er's disease tissue by synchrotron Fourier transform infrared microspectroscopy, Biophys. J. 71 (1996) 1672–1679.
[76] A. Snow, T. Wight, Proteoglycans in the pathogenesis of Alzheimer's disease and other amyloidoses, Neurobiol. Aging 10 (1989) 481–497.
[77] M.B. Pepys, T.W. Rademacher, A.-C. Supavadee, P. Williams, G.E. Noble, W.L. Hutchinson, P.N. Hawkins, S.R. Nelson, J.R. Gallimore, J. Herbert, T. Hutton, R.A. Dwek, Human serum amyloid P component is an invariant constituent of amyloid deposits and has a uniquely homogeneous glycostructure, Proc. Natl. Acad. Sci. USA 91 (1994) 5602–5606.
[78] W.K. Strittmatter, W.J. Huang, L. Dong, G.S. Salvesen, M. Pericak-Vance, D. Schmechel, A.M. Saunders, D. Goldgaber, A. Roses, Binding of human apolipoprotein E to synthetic amyloid β-peptide: Isoform-specific effects for late-onset Alzheimers disease, Proc. Natl. Acad. Sci. USA 90 (1993) 8098–8102.
[79] G. Utermann, The apolipoprotein E connection, Curr. Biol. 4 (1994) 362–365.
[80] C. Abraham, D. Selkoe, H. Potter, Immunochemical identification of the serine protease inhibitor α-1 antichymotrypsin in the brain amyloid deposits of Alzheimer's disease, Cell 52 (1988) 487–501.
[81] P.L. McGeer, E.G. McGeer, The inflammatory response system of brain: Implications for therapy of Alzheimer and other neurodegenerative diseases, Brain Res. Rev. 21 (1995) 195–218.
[82] P. Fraser, J. Nguyen, D. Chin, D. Kirschner, Effects of sulphate ions on Alzheimer β/A4 peptide assemblies for amyloid fibril-proteoglycan interactions, J. Neurochem. 59 (1992) 1531–1540.
[83] K.R. Brunden, N.J. Richter-Cook, N. Chaturvedi, R.C.A. Frederickson, pH dependent binding of synthetic β-amyloid peptides to glycosaminoglycans, J. Neurochem. 61 (1993) 2147–2154.
[84] H. Hamazaki, Ca^{2+}-dependent binding of human serum amyloid P component to Alzheimer's β-amyloid peptide, J. Biol. Chem. 270 (1995) 10392–10394.
[85] J. Emsley, J. White, B. O'Hara, G. Oliva, N. Srinivasan, I. Tickle, T. Blundell, M. Pepys, S. Wood, Structure of pentarmeric human serum amyloid P component, Nature 367 (1994) 338–345.
[86] C. Kinoshita, A. Grewurz, J. Siegel, S. Ying, T. Hugh, J. Coe, R. Gipta, R. Huckman, H. Gerwurz, A protease sensitive site in the proposed Ca^{2+} region of human SAP component and other pentraxins, Protein Sci. 1 (1992) 700–709.
[87] G. Tennent, L. Lovat, M. Pepys, Serum amyloid P component prevents proteolysis of the amyloid fibrils of Alzheimer's disease and systemic amyloidosis, Proc. Natl. Acad. Sci. USA 92 (1995) 4299–4303.
[88] M. LaDu, M. Falduto, A. Manelli, C. Reardon, G. Getz, D. Frail, Isoform-specific binding of apolipoprotein E to β-amyloid, J. Med. Biol. 269 (1994) 23403–23406.
[89] C. Abraham, T. Shirahama, H. Potter, α-1 Antichymotypsin is associated solely with amyloid deposition containing the β-protein. Amyloid and cell localization of α-1 antichymotrypsin, Neurobiol. Aging 11 (1990) 123–129.
[90] P.E. Fraser, J.T. Nguyen, C.R. McLachlan, C.R. Abraham, D.A. Kirschner, α_1-Antichymotrypsin binding to Alzheimer Aβ peptides is sequence specific and induces fibril dissaggregation in vitro, J. Neurochem. 61 (1993) 298–305.
[91] J. Ma, A. Yee, B. Brewer, S. Das, H. Potter, Amyloid-associated proteins α1-antichymotrypsin and apolipoprotein E promote assembly of Alzheimer β-protein into filaments, Nature 372 (1994) 92–94.